Targeted delivery of cisplatin to prostate cancer cells by aptamer functionalized Pt(IV) prodrug-PLGA–PEG nanoparticles

Shanta Dhar[a], Frank X. Gu[b,c], Robert Langer[b,c,d,e], Omid C. Farokhzad[c,f,1], and Stephen J. Lippard[a,d,1]

Departments of [a]Chemistry and [b]Chemical Engineering, [c]MIT-Harvard Center for Cancer Nanotechnology Excellence, [d]Koch Institute for Integrative Cancer Research, and [e]Division of Health Sciences and Technology, Massachusetts Institute of Technology, Cambridge, MA 02139; and [f]Department of Anesthesiology, Brigham and Women's Hospital, Harvard Medical School, 75 Francis St, Boston, MA 02115

Contributed by Stephen J. Lippard, September 17, 2008 (sent for review September 1, 2008)

Cisplatin is used to treat a variety of tumors, but dose limiting toxicities or intrinsic and acquired resistance limit its application in many types of cancer including prostate. We report a unique strategy to deliver cisplatin to prostate cancer cells by constructing Pt(IV)-encapsulated prostate-specific membrane antigen (PSMA) targeted nanoparticles (NPs) of poly(D,L-lactic-*co*-glycolic acid) (PLGA)-poly(ethylene glycol) (PEG)-functionalized controlled release polymers. By using PLGA-*b*-PEG nanoparticles with PSMA targeting aptamers (Apt) on the surface as a vehicle for the platinum(IV) compound *c,t,c*-[Pt(NH$_3$)$_2$(O$_2$CCH$_2$CH$_2$CH$_2$CH$_2$CH$_3$)$_2$Cl$_2$] (1), a lethal dose of cisplatin was delivered specifically to prostate cancer cells. PSMA aptamer targeted delivery of Pt(IV) cargos to PSMA$^+$ LNCaP prostate cancer cells by endocytosis of the nanoparticle vehicles was demonstrated using fluorescence microscopy by colocalization of green fluorescent labeled cholesterol-encapsulated NPs and early endosome marker EEA-1. The choice of linear hexyl chains in 1 was the result of a systematic study to optimize encapsulation and controlled release from the polymer without compromising either feature. Release of cisplatin from the polymeric nanoparticles after reduction of 1 and formation of cisplatin 1,2-intrastrand d(GpG) cross-links on nuclear DNA was confirmed by using a monoclonal antibody for the adduct. A comparison between the cytotoxic activities of Pt(IV)-encapsulated PLGA-*b*-PEG NPs with the PSMA aptamer on the surface (Pt-NP-Apt), cisplatin, and the nontargeted Pt(IV)-encapsulated NPs (Pt-NP) against human prostate PSMA-overexpressing LNCaP and PSMA$^-$ PC3 cancer cells revealed significant differences. The effectiveness of PSMA targeted Pt-NP-Apt nanoparticles against the PSMA$^+$ LNCaP cells is approximately an order of magnitude greater than that of free cisplatin.

DNA cross-link | metals in medicine | PSMA | controlled release

Prostate cancer (PCa) is the most common form of cancer and the second leading cause of death after lung cancer among men in the United States (1). In 2008, there are estimated to be 186,320 domestic new cases and 28,660 deaths by PCa (1). A strategy for treating prostate and other types of cancer involves targeting antigens specific for the tumor of interest. Identification of several prostate antigens offers possible candidates for targeted therapy. The most appealing antigen is the prostate-specific membrane antigen (PSMA) (2, 3). PSMA is abundantly expressed in prostate cancer, its metastatic form, and the hormone-refractory form (4, 5) and the neovasculature of many non-prostate solid tumors (6). PSMA is a type II membrane protein with folate hydrolase activity (7, 8).

The ability of *cis*-diamminedichloroplatinum(II), cisplatin (9, 10), to inhibit the growth of cancer cells by interfering with transcription and other DNA-mediated cellular functions has been elucidated over the past 30 years. Cisplatin is highly effective against several forms of cancer, most notably testicular tumors, and it is also commonly used to treat breast, ovarian, bladder, lung, and head and neck cancer. Prostate cancer is resistant to cisplatin chemotherapy due to poor targeting and the development of resistance (11). To overcome the latter, the cisplatin dosage can be elevated, but not without serious side effects. Because cisplatin is the most potent member of the Pt anticancer drug family, its potential use in prostate cancer is attractive. We therefore devised a strategy for cisplatin therapy in prostate cancer based on mechanisms that target critical molecular pathways of prostate tumors and that employ platinum chemistry and delivery vehicles for such targeting.

Targeted controlled release drug delivery systems have the potential to induce dramatic and durable clinical responses. Designing drug delivery systems that target specific sites with controlled release of the drug over a period is challenging (12–14). Controlled release polymeric nanoparticles (NPs) are a powerful technology in this regard (15–18). With surface engineering, it is possible to introduce ligands, such as peptides, antibodies, or nucleic acid aptamers, that can target NPs to a cancer cell of interest. Encapsulation of a drug within the interior of the particle protects it from the external environment, increasing blood circulation time of the active dose before reaching its target. A platinum complex encapsulated within nanoparticles administered to a patient will be protected from body fluids before reaching the target cell and its nuclear DNA, and the body will also be isolated from undesired chemical consequences of the drug.

NPs based on biodegradable, biocompatible, and FDA-approved components are of interest because their use facilitates their future transition into clinical trials. NPs derived from poly(D,L-lactic-*co*-glycolic acid) (PLGA) as the controlled release polymer system are an excellent choice since their safety in clinic is well established (13). Poly(ethylene glycol) (PEG)-functionalized PLGA NPs are especially desirable because pegylated polymeric NPs have significantly reduced systemic clearance compared with similar particles without PEG (19, 20). A number of FDA approved drugs in clinical practice use PEG for improved pharmaceutical properties (21).

In this study, we applied a Pt(IV)-prodrug approach previously employed in our laboratory (22–25) to deliver cisplatin, using PSMA targeted pegylated PLGA NPs as the vehicle (26). Encapsulation of cisplatin into polymeric NPs is a challenge

Author contributions: S.D., R.L., O.C.F., and S.J.L. designed research; S.D. and F.X.G. performed research; S.D. contributed new reagents/analytic tools; S.D., F.X.G., O.C.F., and S.J.L. analyzed data; and S.D. and S.J.L. wrote the paper.

The authors declare no conflict of interest.

Data deposition: The atomic coordinates have been deposited in the Cambridge Structural Database, Cambridge Crystallographic Data Centre, Cambridge CB2 1EZ, United Kingdom (CSD reference no. CCDC 705067).

[1]To whom correspondence may be addressed. E-mail: lippard@mit.edu or ofarokhzad@zeus.bwh.harvard.edu.

This article contains supporting information online at www.pnas.org/cgi/content/full/0809154105/DCSupplemental.

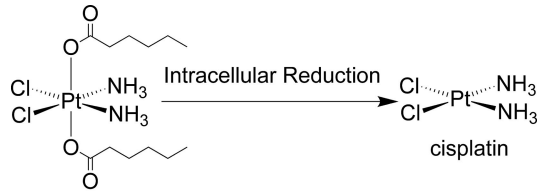

1

Scheme 1. Chemical structure of the hydrophobic platinum(IV) compound **1** and the chemistry by which the active drug, cisplatin is released, after reduction in the cell.

because of its physico-chemical properties (27, 28). Cisplatin is insoluble in organic solvents, and its partial solubility in water makes it difficult to obtain cisplatin-encapsulated-PLGA sustained-release systems that maintain adequate concentrations for long time periods (28). A recent effort to prepare such a construct by the double emulsion method resulted in large particles, which tend to sequester in the liver and spleen (29), with encapsulated cisplatin exhibiting lower cytotoxicity than that of the free drug (30). Particles >200 nm are generally ineffective in vivo. In another report, the in vitro anticancer activity of cisplatin-encapsulated PLGA-mPEG nanoparticles was investigated against prostate cancer LNCaP cells, but the nanoparticles loaded with cisplatin showed comparable or lower activity compared with that of free cisplatin (31). The prodrug approach, where cisplatin is released from a Pt(IV) precursor, overcomes the problems associated with cisplatin encapsulation, and allows a cell targeting moiety to deliver a lethal dose of cisplatin upon intracellular reduction (22–25). Because the interior of nanoparticles is more hydrophobic than their surface, we prepared a Pt(IV) compound *c,t,c* $[Pt(NH_3)_2(O_2CCH_2CH_2CH_2CH_2CH_3)_2Cl_2]$ (**1**, Scheme 1) having alkyl chains at the axial positions. Encapsulation of this molecule into pegylated PLGA nanoparticle bioconjugates that bind to the PSMA protein on the surface of prostate cancer cells for targeted delivery of the Pt(IV) prodrug led to release of cisplatin upon intracellular reduction (Scheme 1). Although related constructs were devised many years ago (32), the choice of the linear hexyl chains in **1** was the result of a systematic study to optimize encapsulation and controlled release from the polymer without compromising either feature. For targeting, we used the A10 2′-fluoropyrimidine RNA aptamer, which recognizes the extracellular domain of PSMA (A10 PSMA Apt) (33) to functionalize the surface of our Pt(IV)-encapsulated pegylated PLGA NPs. The results of these experiments are described here.

Results and Discussion

Synthesis and Characterization of 1. The interior of nanoparticles is more hydrophobic than their surface. Initial efforts to obtain the required hydrophobicity included synthesis of a Pt(IV) derivative of cisplatin having with adamantyl groups at the axial positions, but this compound was insoluble in acetonitrile. To obtain a platinum complex with sufficient hydrophobicity for encapsulation in PLGA-*b*-PEG NPs, we ultimately synthesized *c,t,c*-$[Pt(NH_3)_2(O_2CCH_2CH_2CH_2CH_2CH_3)_2Cl_2]$ (**1**) (Scheme 1) (22, 32). The structure of **1** was confirmed by spectroscopic [supporting information (SI) Fig. S1], analytical, and X-ray crystallographic methods. Details of the structure are available in Table S1 and Fig. S2. Synthesis of Pt(IV)-encapsulated nanoparticles requires that the Pt(IV) host be sufficiently soluble in organic solvents like acetonitrile and DMF. Compound **1** dissolves in acetonitrile (10 mg/ml), making it a suitable candidate for encapsulation.

Development of Pt(IV)-Encapsulated, A10 PSMA Apt Funtionalized NPs (Pt-NP-Apt). PLGA-COOH and NH_2-PEG_{3400}-COOH polymers were used to prepare a PLGA-*b*-PEG copolymer with terminal carboxylic acid groups (PLGA-*b*-PEG-COOH) (34). PLGA-COOH was converted to its succinimide by using 1-ethyl-3-[3-dimethylaminopropyl]carbodiimide hydrochloride (EDC) and *N*-hydroxysuccinimide (NHS), which was then allowed to react with NH_2-PEG-COOH. We used a nanoprecipitation method (35) to encapsulate **1** within a PLGA-*b*-PEG block copolymer having a terminal carboxylic acid group (PLGA-*b*-PEG-COOH) (Fig. 1*A*). The properties of the encapsulated nanoparticle were characterized by dynamic light scattering to give the size and polydispersity of each preparation. To optimize the size and loading, a series of encapsulated NPs were prepared, varying the weight percentage of **1** to polymer and by using PLGA of various molecular masses. In this way, we found PLGA of inherent viscosity 0.69 dL/g in hexafluoroisopropanol to afford the most suitable encapsulated NPs.

The loading efficiencies of **1** at various added weight-percentage values of Pt(IV) to polymer are shown in Fig. 1*B*. The polydispersity of the particles increases with the percentage loading of **1** (Table 1). The size of the particles also increases with percentage loading (Table 1). For all studies, we used encapsulated particles having a ≈6% loading and a size of ≈140 nm (Fig. 1*C*). We modified the surface of **1**-encapsulated NPs with the A10 PSMA Apt. The presence of targeting moieties on the surface of particles allows it to differentially bind and become internalized by PCa cells. The 5′ amino groups of the aptamer were conjugated to the carboxylate groups of the NPs surface using an amide coupling reagent. Conjugation of the A10 PSMA Apt on the surface of NPs was confirmed by agarose gel electrophoresis (Fig. S3*a*).

In Vitro Controlled Release of 1 from Encapsulated NPs. We next studied the controlled release kinetics of the Pt(IV) complex **1** from the NPs, a necessary property for anticancer activity (36). Doxorubicin covalently linked to PLGA (37) or poly(aspartic acid) (38) displays very little or no activity because the absence of a hydrolyzable linker precluded its release. A more recent study in which doxorubicin was conjugated to PLGA by a hydrolyzable carbamate linkage showed a sustained release drug profile from this nanocell delivery system (39). The platinum(IV) compound is physically dispersed by encapsulation throughout the hydrophobic core of the PLGA-*b*-PEG NPs. Typically, except for an initial burst, release from polymeric NPs is a slow, diffusion-controlled process that also depends on the rate of polymer biodegradation (40). We studied release by dialyzing the Pt-encapsulated NPs against 20 L of PBS at pH 7.4 and 37 °C to mimic physiological conditions. The amount of platinum released from the particles was measured by atomic absorption spectroscopy (AAS). The controlled release of platinum from the NPs is shown in Fig. 2. An initial burst release during the first 2 h represents only 12% of the total platinum. The dormant period lasts ≈14 h (49%). Thereafter, a period of controlled platinum release occurs, reaching a value of 66% after 24 h. Such controlled release of Pt(IV) from the NPs extended over 60 h. These physicochemical properties confirmed our choice of the platinum(IV) compound **1**, having linear hexyl chains in the axial positions, as optimal for building a sustained-release platinum-nanoparticle conjugate.

The identity of the platinum species released from the polymeric nanoparticles was determined by electrospray ionization mass spectrometry (ESI-MS). ESI-MS analysis of the PBS dialysate from the Pt-NP dialysis experiment revealed a peak at 553.5 (Fig. S3*b*) corresponding to the sodium adduct of **1** $[(M+Na^+)_{calcd}$ 553.34]. This result indicates that the acidic environment inside the NPs is insufficient to promote conversion of **1** to its platinum(II) form cisplatin, assuring that **1**

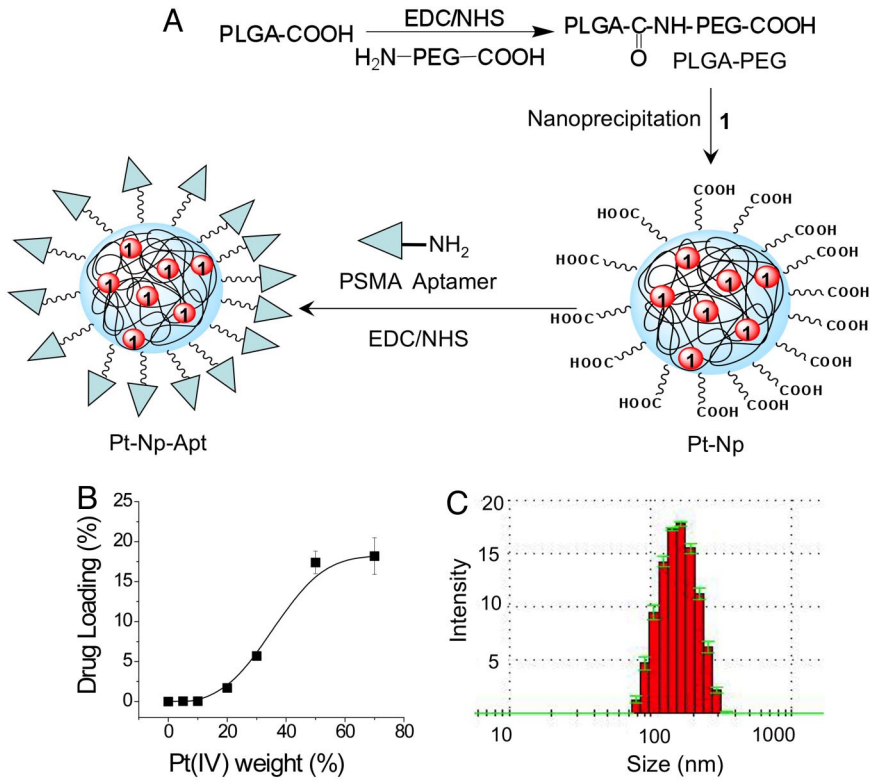

Fig. 1. Construction and properties of aptamer-functionalized Pt(IV) nanoparticles. (*A*) Synthesis of Pt(IV)-encapsulated PLGA-*b*-PEG-COOH nanoparticles by nanoprecipitation and conjugation of PSMA aptamer to NP. (*B*) Loading of **1** in the PLGA-*b*-PEG-COOH nanoparticles. (*C*) Size of the Pt(IV)-encapsulated nanoparticles.

remains in its unmodified form after entrapment in the particles, making them a valuable delivery vehicle for Pt(IV) compounds. We also investigated the redox potential for reduction of **1** at various pH values. Electrochemical analyses revealed that **1** displays an irreversible cyclic voltammetric response for the Pt(IV)/Pt(II) couple near −0.805 V vs. NHE in MeCN and approximately −0.233 V and −0.243 V vs. NHE in a 1:4 mixture of DMF-sodium phosphate buffer at pH 7.4 and 6.0, respectively (Figs. S4–S6). These reduction potentials suggest that the compound should be sufficiently stable toward reduction in the bloodstream during delivery to the target cell by the nanoparticles.

Targeted Endocytosis and Endosomal Localization of Pt(IV)-Encapsulated A10 PSMA Apt Functionalized NPs. Because nanoparticle uptake into cells occurs by various processes, including phagocytosis and endocytosis, we performed studies to investigate the uptake mechanism of our conjugate. Visible evidence of targeted uptake of Pt-NP-Apt by PSMA-expressing prostate cancer cells via endocytosis was obtained by fluorescence microscopy with the use of NPs containing both **1** and a green fluorescent labeled cholesterol derivative, 22-NBD-cholesterol. PSMA is highly expressed on virtually all prostate cancer cells and is currently the focus of several diagnostic and therapeutic strategies (41, 42). LNCaP human prostate epithelial cells express a high level of PSMA protein on their cell surface and represent a good model for in vitro and in vivo prostate cancer studies. PC3 human prostate epithelial cells normally do not express any detectable levels of the PSMA protein. We examined LNCaP ($PSMA^+$) and PC3 ($PSMA^-$) cells to measure the enhanced uptake of the **1**-encapsulated PSMA-targeted NPs against LNCaP but not PC3 cells. As shown in Fig. 3, incubation of LNCaP cells with the Pt(IV) and

Table 1. Nanoparticle characterization

Weight of **1** used for encapsulation, %	Loading, %	Mean size, nm	Polydispersity index
5	0.05	132 ± 3.4	0.171 ± 0.02
10	0.05	131 ± 0.5	0.186 ± 0.02
20	1.7	135 ± 3.4	0.205 ± 0.03
30	5.7	137 ± 4.6	0.259 ± 0.04
50	17.4	167 ± 4.3	0.444 ± 0.06
70	18.4	172 ± 3.4	0.479 ± 0.17

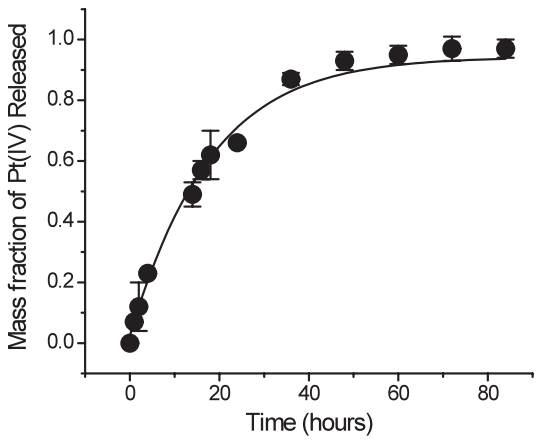

Fig. 2. *In vitro* release kinetics of encapsulated Pt(IV) compound **1** from PLGA-*b*-PEG nanoparticles in PBS (pH 7.4) at 37 °C.

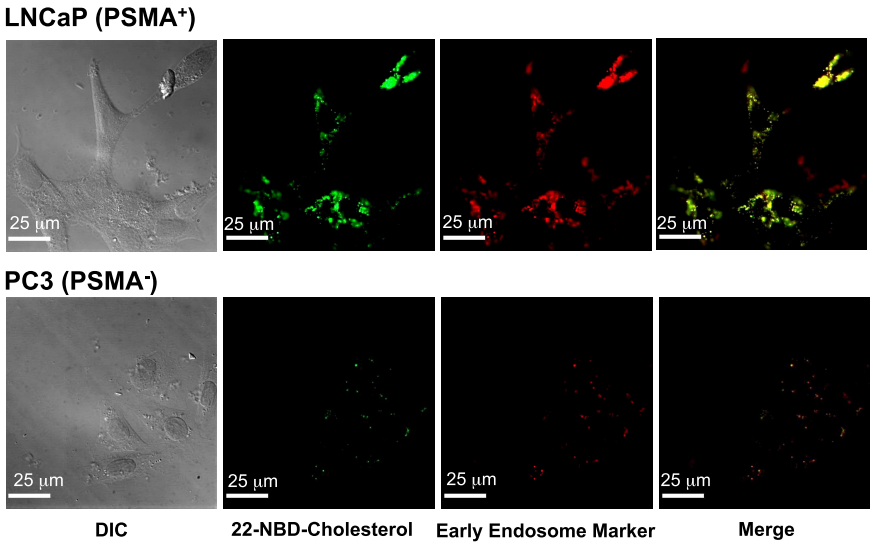

Fig. 3. Detection of endosome formation and cellular uptake of Pt-NP-Apt in LNCaP cells by fluorescence microscopy. Green fluorescent 22-NBD-cholesterol and **1** were encapsulated in the PLGA-*b*-PEG nanoparticles and PSMA aptamers were conjugated to the surface of the particles. The early endosomes were visualized in red by using the early endosome marker EEA-1.

cholesterol-coencapsulated PSMA-targeted NPs for 2h and use of the early endosome marker EEA-1 antibody revealed complete internalization of the nanoparticles by receptor mediated endocytosis. In contrast, no significant accumulation of the NPs was observed in the PC3 cells, further confirming the differential binding and uptake of targeted NPs by receptor mediated endocytosis. From the release study mentioned above, we observed only 12% of total Pt(IV) to be released after 2 h in PBS at 37 °C, indicating that complete internalization of the particles within 2 h is sufficient to deliver almost all their platinum(IV) content to the cells.

In Vitro Cellular Cytotoxicity Assays. We performed a series of in vitro cytotoxicity assays to evaluate the anti-cancer potential of platinum(IV)-encapsulated targeted nanoparticles, using LNCaP ($PSMA^+$) and PC3 ($PSMA^-$) cells and directly comparing its efficacy to that of cisplatin. As shown in Fig. 4 *A* and *B*, Pt-NP-Apt are highly cytotoxic to the LNCaP cells, which express the PSMA protein on their surface, having an IC_{50} value of 0.03 μM. Under the same conditions, the nontargeted particles (Pt-NP) have an IC_{50} value of 0.13 μM, and for cisplatin the value with these cells is 2.4 μM, ~2 orders of magnitude less effective. The IC_{50} of Pt-NP-Apt increases to 0.11 μM in the $PSMA^-$ PC3 cells. The IC_{50} value of the nontargeted particles (Pt-Np) with PC3 cells is 0.12 μM, comparable to that of the targeted Pt-NP-Apt particles and consistent with the lack of PSMA expression in these cells. Free cisplatin has an IC_{50} of 0.18 μM with PC3 cells. Compared with these values, the cytotoxicity of the parent prodrug **1** is insignificant ($IC_{50} > 1.0$ μM) in both LNCaP and PC3 cells. These results demonstrate aptamer-targeted delivery of a Pt(IV) prodrug to PSMA-expressing LNCaP cells by a nanoparticle delivery system. The PSMA aptamer-targeted Pt(IV)-encapsulated PLGA-*b*-PEG nanoparticles are 80 times more toxic than free cisplatin in the $PSMA^+$ LNCaP cells, indicating the potential of these nanoparticles to treat human prostate cancer.

Visualization of Cisplatin 1,2-d(GpG) Intrastrand Adduct by Immunofluorescence. The anticancer activity of cisplatin is based on the formation of intrastrand cross-links on nuclear DNA (9). Several such adducts have been structurally identified, of which the 1,2-guanine–guanine intrastrand cross-link *cis*-{$Pt(NH_3)_2d(GpG)$} represents >65% of total DNA platination. We used a monoclonal antibody R-C18 specific for this adduct (43) to learn whether cisplatin released from reduction

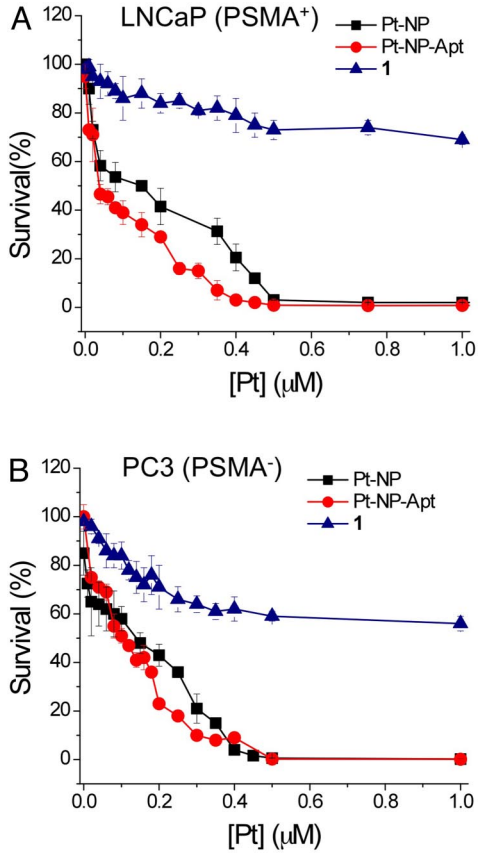

Fig. 4. Cytotoxicity profiles of PSMA aptamer-targeted Pt(IV)-encapsulated PLGA-*b*-PEG nanoparticles (Pt-NP-Apt) (red circles), nontargeted nanoparticles (Pt-NP) (black squares), and compound **1** (blue triangles) with (*A*) $PSMA^+$ LNCaP cells and (*B*) $PSMA^-$ PC3 cells after 72 h as determined by the MTT assay.

of **1** forms this cross-link with nuclear DNA. After a 12-h incubation of $PSMA^+$, LNCaP cells with Pt-NP-Apt, formation of the 1,2-d(GpG) intrastrand cross-links was observed by antibody-derived green fluorescence in the nuclei of these cells (Fig. S7). These results confirm the complete delivery pathway of cisplatin via **1** to PSMA-expressing prostate cancer cells through targeted nanoparticle endocytosis followed by reduction of **1** to deliver a lethal dose of the drug, which forms its signature adduct on nuclear DNA in the cell.

Comparison to Related Work. While this article was in preparation, a related report appeared in which the previously described Pt(IV) compound, *c,t,c*-$[Pt(NH_3)_2(succinate)_2Cl_2]$ (22), was conjugated to nanoscale coordination polymers constructed from Tb^{3+} (44). Although the system is unstable in water and stabilization required encapsulation in shells of amorphous silica, the targeted NPs with c(RGDfK) on the surface exhibited IC_{50} values of 9.7–11.9 μM with $\alpha_v\beta_3$ integrin-up-regulated HT-29 cells. These values are comparable to that of free cisplatin (13.0 μM).

Summary. In this study, a hydrophobic platinum(IV) compound **1** was synthesized for encapsulation in the PLGA-*b*-PEG nanoparticles by the nanoprecipitation method, resulting in moderately highly loaded particles of suitable size for delivering cisplatin to prostate cancer cells. The particles were targeted to PSMA, which is overexpressed in prostate cancer, by decorating the surface of the particles with the A10 aptamer that specifically binds to the extracellular domain of PSMA. The aptamer-facilitated cellular uptake of the Pt(IV)-encapsulated nanoparticles by $PSMA^+$ LNCaP cells via endocytosis was demonstrated using an antibody specific for endosome formation. The aptamer-derivatized Pt(IV)-encapsulated nanoparticles are significantly superior to cisplatin or nontargeted nanoparticles against the LNCaP cells. Cisplatin produced by reductive release from the nanoparticles forms 1,2-d(GpG) intrastrand cross-links at the nuclear DNA of the LNCaP cells. The strategy of delivering a Pt(IV) compound selectively to prostate cancer cells opens up avenues for systemic targeted therapy against this cancer using platinum drugs. More broadly, by targeting other tumor-specific antigens, using similarly engineered nanoparticles, it may be possible to selectively deliver a therapeutic dose of platinum drugs to a myriad of cancers. Further studies with relevant animal models are needed.

Materials and Methods

Potassium tetrachloroplatinate(II) was obtained as a gift from Engelhard Corporation (now BASF). Cisplatin (45) and *c,c,t*-$[Pt(NH_3)_2Cl_2(OH)_2]$ (46) were synthesized as previously described. *N*-hydroxysuccinimide (NHS), 1-ethyl-3-[3-dimethylaminopropyl]carbodiimide hydrochloride (EDC), paraformaldehyde, hydroxyethyl starch (HEAS), and hexanoic anhydride were purchased from Aldrich. PLGA with acid end groups was purchased from Adsorbable Polymers International. A PEG polymer of molecular weight 3,400 with a terminal amine and carboxylic group (NH_2-PEG-COOH) was custom synthesized (Nektar Therapeutics). The RNA aptamer with the sequence 5′-NH_2-spacer GGGAGGACGAUGCGGAUCAGCCAUGUUUA-CGUCACUCCUUGUCAAUCCUCAUCGGCiT-3′ containing 2′-fluoro pyrimidines, a 3′-inverted T cap, and a 5′-amino group attached by a hexaethyleneglycol spacer was custom synthesized by RNA-TEC. Green fluorescent dye, 22-NBD-cholesterol, was purchased from Invitrogen. Early endosomal marker, mouse monoclonal EEA-1, was obtained from Abcam. The secondary antibody for EEA-1, Cy5 goat anti-mouse antibody, was purchased from Invitrogen. For detection of the cisplatin 1,2-d(GpG) intrastrand adduct, we used a monoclonal adduct specific antibody R-C18 kindly provided by J. Thomale (University of Essen, Duisburg-Essen, Germany). FITC labeled secondary antibody rabbit anti-(rat Ig) was obtained from Invitrogen. Specific adhesion slides for immunofluorescence were purchased from Squarix Biotechnology. ^1H, ^{13}C, and ^{195}Pt NMR spectra were recorded on a Bruker AVANCE-400 spectrometer with a Spectro Spin superconducting magnet in the MIT Department of Chemistry Instrumentation Facility. ESI-MS analyses were performed on an Agilent 1100 series instrument. Atomic absorption spectroscopic measurements were taken on a Perkin–Elmer AAnalyst 300 spectrometer. Fluorescence imaging studies were performed with an Axiovert 200M inverted epifluorescence microscope (Zeiss) equipped with an EM-CCD digital camera C9100 (Hamamatsu). An X-Cite 120 metal-halide lamp (EXFO) was used as the light source. The microscope was operated with Volocity software (Improvision). Electrochemical measurements were performed at 25 °C on a VersaSTAT3 Princeton Applied Research electrochemical analyzer with V3-Studio electrochemical analysis software, using a 3-electrode set-up comprising a glassy carbon working electrode, platinum wire auxiliary electrode, and a Ag/AgCl reference electrode. The electrochemical data were uncorrected for junction potentials. Tetra-*n*-butyl ammonium hexafluorophosphate and KCl were used as supporting electrolytes.

Synthesis of *c,c,t*-$[Pt(NH_3)_2Cl_2(O_2CCH_2CH_2CH_2CH_2CH_3)_2]$ (1). To a solution of *c,c,t*-$[Pt(NH_3)_2Cl_2(OH)_2]$ (0.69 g, 2.05 mmol) in DMSO (10 mL) was added hexanoic anhydride (0.90 g, 4.2 mmol), and the reaction mixture was stirred at room temperature for 48 h. Water was added to the mixture to precipitate a light yellow solid, which was dissolved in acetonitrile. Rotary evaporation of the acetonitrile solution resulted a yellow solid, which was washed several times with diethyl ether and dried. Compound **1** was isolated in 42% (0.6 g) yield. ^1H NMR (DMSO-d_6) δ 6.52 (s, 6H), 2.21–2.17 (t, J = 8 Hz, 4H), 1.48–1.41 (m, 4H), 1.30–1.19 (m, 8H), 0.87–0.83 (t, J = 8 Hz, 6H); ^{13}C NMR (DMSO-d_6) δ 180.88, 35.65, 30.87, 25.14, 22.00, 13.93; ^{195}Pt NMR (DMSO-d_6): δ 1217.79 ppm. Anal: Calcd for $C_{12}H_{28}Cl_2N_2O_4Pt$: C, 27.18; H, 5.32; N, 5.28. Found: C, 27.07; H, 5.40; N, 5.19.

Synthesis of Pt(IV)-Encapsulated NPs (Pt-NPs). Copolymer PLGA-*b*-PEG containing terminal carboxylate groups was synthesized by the amide coupling of COOH-PEG-NH_2 to PLGA-COOH in methylene chloride as described in ref. 34. Pt(IV)-encapsulated NPs were prepared by using the nanoprecipitation method. PLGA-*b*-PEG (10 mg/ml) and **1** at varying concentrations with respect to the polymer concentration were dissolved in acetonitrile. This mixture was slowly added to water over a period of 10 min. The NPs formed were stirred at room temperature for 3 h and then washed 3 times, using Amicon ultracentrifugation filtration membranes with a molecular mass cutoff of 100 kDa. The NP size was obtained by quasi-electric laser light scattering by using a ZetaPALS dynamic light-scattering detector (15 mW laser, incident beam = 676 nm, Brookhaven Instruments). The Pt content in the NPs was measured by atomic absorption spectroscopy.

Conjugation of Apt on the Surface of Pt(IV)-Encapsulated NPs (Pt-NP-Apt). A Pt(IV)-encapsulated PLGA-b-PEG-COOH NP suspension in DNase RNase-free water (≈10 μg/μL) was treated with 400 mM EDC and 100 mM NHS for 15 min at room temperature with mild agitation to give the corresponding NHS-ester. The NHS-activated NPs were washed twice using Amicon ultracentrifugation filtration membrane with a molecular mass cutoff of 100 kDa to remove unreacted NHS and conjugated to 5′-NH_2-modified A10 PSMA Apt of 2% weight compared with polymer concentration for 2 h at room temperature with gentle stirring. The resulting Apt conjugated Pt(IV)-encapsulated NPs, Pt-NP-Apt, were washed 3 times with DNase RNase-free water using Amicon filters and resuspended in PBS.

Release of 1 from the PLGA-b-PEG NPs. A suspension of Pt(IV)-encapsulated particles in water was aliquotted (100 μL) into several semipermeable minidialysis tubes (molecular mass cutoff 100 kDa; Pierce) and dialyzed against 20 L PBS (pH 7.4) at 37 °C. At a predetermined time, an aliquot of the NP suspension was removed, dissolved in acetonitrile, and the platinum content was determined by AAS.

Endocytosis of Apt-Targeted Pt(IV)-Encapsulated PLGA-b-PEG NPs. MTT Cell Proliferation Assay. Monoclonal Antibody Detection of cis-$\{Pt(NH_3)_2\}^{2+}$ Intrastrand d(GpG) Cross-link. Experimental details for these studies are available in *SI Methods*.

ACKNOWLEDGMENTS. This work was supported by National Cancer Institute Grants CA34992 (to S.J.L.) and CA119349 (to O.C.F. and R.L.), the National Institute of Biomedical Imaging and Bioengineering Grant EB003647 (to O.C.F.), a Koch–Prostate Cancer Foundation Award in Nanotherapeutics (to O.C.F. and R.L.), a postdoctoral fellowship from the Anna Fuller Fund for Molecular Oncology (S.D.), and a postdoctoral fellowship from the Canadian Natural Sciences and Engineering Research Council (F.G.).

1. Jemal A, *et al.* (2008) Cancer statistics, 2008. *CA Cancer J Clin* 58:71–96.
2. Israeli RS, Powell CT, Fair WR, Heston WDW (1993) Molecular cloning of a complementary DNA encoding a prostate-specific membrane antigen. *Cancer Res* 53:227–230.
3. Murphy GP, *et al.* (1998) Current evaluation of the tissue localization and diagnostic utility of prostate specific membrane antigen. *Cancer* 83:2259–2269.
4. Kawakami M, Nakayama J (1997) Enhanced expression of prostate-specific membrane antigen gene in prostate cancer as revealed by in situ hybridization. *Cancer Res* 57:2321–2324.
5. Wright GL, Jr, *et al.* (1996) Upregulation of prostate-specific membrane antigen after androgen-deprivation therapy. *Urology* 48:326–334.
6. Chang SS, *et al.* (1999) Five different anti-prostate-specific membrane antigen (PSMA) antibodies confirm PSMA expression in tumor-associated neovasculature. *Cancer Res* 59:3192–3198.
7. Pinto JT, *et al.* (1996) Prostate-specific membrane antigen: A novel folate hydrolase in human prostatic carcinoma cells. *Clin* Cancer Res 2:1445–1451.
8. Rawlings ND, O'Brien E, Barrett AJ (2002) MEROPS: The protease database. *Nucleic Acids Res* 30:343–346.
9. Jamieson ER, Lippard SJ (1999) Structure, recognition, and processing of cisplatin-DNA adducts. *Chem Rev* 99:2467–2498.
10. Rosenberg B, VanCamp L, Trosko JE, Mansour VH (1969) Platinum compounds: A new class of potent antitumour agents. *Nature* 222:385–386.
11. Nomura T, Mimata H (2007) Molecular mechanisms of cisplatin resistance in prostate cancer cells. *Cancer Drug Resistance Perspectives*, ed Torres LS, (Nova Science Publishers, New York), Vol. 121, pp 95–105.
12. Ferrari M (2005) Cancer nanotechnology: Opportunities and challenges. *Nat Rev Cancer* 5:161–171.
13. Langer R (1998) Drug delivery and targeting. *Nature* 392:5–10.
14. Langer R (2001) Drugs on target. *Science* 293:58–59.
15. Brannon-Peppas L, Blanchette JO (2004) Nanoparticle and targeted systems for cancer therapy. *Adv Drug Delivery Rev* 56:1649–1659.
16. Brigger I, Dubernet C, Couvreur P (2002) Nanoparticles in cancer therapy and diagnosis. *Adv Drug Delivery Rev* 54:631–651.
17. Zhang L, *et al.* (2008) Nanoparticles in medicine: Therapeutic applications and developments. *Clin Pharmacol Ther* 83:761–769.
18. LaVan DA, McGuire T, Langer R (2003) Small-scale systems for in vivo drug delivery. *Nat Biotechnol* 21:1184–1191.
19. Alexis F, Pridgen E, Molnar LK, Farokhzad OC (2008) Factors affecting the clearance and biodistribution of polymeric nanoparticles. *Mol Pharm* 5:505–515.
20. Gref R, *et al.* (1994) Biodegradable long-circulating polymer nanospheres. *Science* 263:1600–1603.
21. Fishburn CS (2008) The pharmacology of PEGylation: Balancing PD with PK to generate novel therapeutics. *J Pharm Sci* 97:4167–4183.
22. Barnes KR, Kutikov A, Lippard SJ (2004) Synthesis, characterization, and cytotoxicity of a series of estrogen-tethered platinum(IV) complexes. *Chem Biol* 11:557–564.
23. Feazell RP, Nakayama-Ratchford N, Dai H, Lippard SJ (2007) Soluble single-walled carbon nanotubes as longboat delivery systems for platinum(IV) anticancer drug design. *J Am Chem Soc* 129:8438–8439.
24. Dhar S, *et al.* (2008) Targeted single-wall carbon nanotube-mediated Pt(IV) prodrug delivery using folate as a homing device. *J Am Chem Soc* 130:11467–11476.
25. Mukhopadhyay S, *et al.* (2008) Conjugated platinum(IV)-peptide complexes for targeting angiogenic tumor vasculature. *Bioconjugate Chem* 19:39–49.
26. Farokhzad OC, *et al.* (2004) Nanoparticle-aptamer bioconjugates: A new approach for targeting prostate cancer cells. *Cancer Res* 64:7668–7672.
27. Avgoustakis K, *et al.* (2002) PLGA-mPEG nanoparticles of cisplatin: In vitro nanoparticle degradation, in vitro drug release and in vivo drug residence in blood properties. *J Controlled Release* 79:123–135.
28. Fujiyama J, *et al.* (2003) Cisplatin incorporated in microspheres: Development and fundamental studies for its clinical application. *J Controlled Release* 89:397–408.
29. Stolnik S, *et al.* (2001) Polylactide-poly(ethylene glycol) micellar-like particles as potential drug carriers: Production, colloidal properties and biological performance. *J Drug Targeting* 9:361–378.
30. Moreno D, *et al.* (2008) Characterization of cisplatin cytotoxicity delivered from PLGA-systems. *Eur J Pharm Biopharm* 68:503–512.
31. Gryparis EC, Hatziapostolou M, Papadimitriou E, Avgoustakis K (2007) Anticancer activity of cisplatin-loaded PLGA-mPEG nanoparticles on LNCaP prostate cancer cells. *Eur J Pharm Biopharm* 67:1–8.
32. Giandomenico CM, *et al.* (1995) Carboxylation of kinetically inert platinum(IV) hydroxy complexes. An entrée into orally active platinum(IV) antitumor agents. *Inorg Chem* 34:1015–1021.
33. Lupold SE, Hicke BJ, Lin Y, Coffey DS (2002) Identification and characterization of nuclease-stabilized RNA molecules that bind human prostate cancer cells via the prostate-specific membrane antigen. *Cancer Res* 62:4029–4033.
34. Farokhzad OC, *et al.* (2006) Targeted nanoparticle-aptamer bioconjugates for cancer chemotherapy in vivo. *Proc Natl Acad Sci USA* 103:6315–6320.
35. Chorny M, Fishbein I, Danenberg HD, Golomb G (2002) Lipophilic drug loaded nanospheres prepared by nanoprecipitation: Effect of formulation variables on size, drug recovery and release kinetics. *J Controlled Release* 83:389–400.
36. Kopecek J, *et al.* (2001) Water soluble polymers in tumor targeted delivery. *J Controlled Release* 74:147–158.
37. Yoo HS, Lee KH, Oh JE, Park TG (2000) In vitro and in vivo antitumor activities of nanoparticles based on doxorubicin-PLGA conjugates. *J Controlled Release* 68:419–431.
38. Yokoyama M, *et al.* (1998) Characterization of physical entrapment and chemical conjugation of adriamycin in polymeric micelles and their design for in vivo delivery to a solid tumor. *J Controlled Release* 50:79–92.
39. Sengupta S, *et al.* (2005) Temporal targeting of tumor cells and neovasculature with a nanoscale delivery system. *Nature* 436:568–572.
40. Zhang Z, Feng S-S (2006) In vitro investigation on poly(lactide)-Tween 80 copolymer nanoparticles fabricated by dialysis method for chemotherapy. *Biomacromolecules* 7:1139–1146.
41. Milowsky MI, *et al.* (2007) Vascular targeted therapy with anti-prostate-specific membrane antigen monoclonal antibody J591 in advanced solid tumors. *J Clin Oncol* 25:540–547.
42. Quintana JC, Blend MJ (2000) The dual-isotope ProstaScint imaging procedure: Clinical experience and staging results in 145 patients. *Clin Nucl Med* 25:33–40.
43. Liedert B, Pluim D, Schellens J, Thomale J (2006) Adduct-specific monoclonal antibodies for the measurement of cisplatin-induced DNA lesions in individual cell nuclei. *Nucleic Acids Res* 34:e47.
44. Rieter WJ, Pott KM, Taylor KML, Lin W (2008) Nanoscale coordination polymers for platinum-based anticancer drug delivery. *J Am Chem Soc* 130:11584–11585.
45. Dhara SC (1970) A rapid method for the synthesis of cis-[Pt(NH3)2Cl2]. *Indian J Chem* 8:193–194.
46. Hall MD, *et al.* (2003) The cellular distribution and oxidation state of platinum(II) and platinum(IV) antitumour complexes in cancer cells. *J Biol Inorg Chem* 8:726–732.